JOURNAL OF GEOPHYSICAL RESEARCH, VOL. 105, NO. B2, PAGES 2679–2697, FEBRUARY 10, 2000

Origin of intraplate volcanoes from guyot heights and oceanic paleodepth

Jacqueline Caplan-Auerbach, Fred Duennebier, and Garrett Ito

Department of Geology and Geophysics, University of Hawaii at Manoa, Honolulu

Abstract. The height of a guyot as measured from the surrounding regional sea floor to the volcano's slope break records the water depth at the time the guyot submerged. Thus guyot heights may be used as indicators of the paleodepth of the surrounding ocean floor. We compile data on the heights of 68 intraplate guyots and atolls in the Pacific Ocean as well as 46 volcanic islands in the Pacific, Atlantic, and Indian Oceans. We find that guyot heights generally increase with the age of the lithosphere upon which they were emplaced, although there is a large amount of scatter. In nearly all cases, seamount height, and thus seafloor paleodepth, is less than expected of normal seafloor. These results suggest that most of the volcanoes in this study formed on anomalously shallow seafloor, consistent with formation at hotspots. To characterize thermal anomalies associated with these hotspot swells, we model guyot heights by calculating the isostatic uplift predicted for normal lithosphere that has been partly reheated and is underlain by anomalously hot mantle. This model is able to explain the anomalous water depth at most of the seamounts with hotspot thermal anomalies of 100°-300°C. The heights of a few volcanic chains, however, are not anomalously low, suggesting that these volcanoes are not associated with hotspots. In addition, the observed trend of Hawaiian-Emperor guyot heights as well as the subdued morphology and gravity signature of the oldest Emperor seamounts supports our hypothesis that Cretaceous age Meiji seamount may have formed on or near a spreading center.

1. Introduction

The study of guyots can be traced to 1946 when H. Hess identified these flat-topped features as eroded islands now submerged beneath the ocean [*Hess*, 1946]. Strictly, any seamount with a flat top may be termed a guyot, but in this paper we consider only those guyots that have undergone subaerial erosion, resulting in a relatively small amount of surficial relief. For these guyots the height from the seafloor to the volcano's erosional horizon should equal the depth of the surrounding seafloor at the location and time of submergence. This concept has been used by a number of researchers to investigate paleo-seafloor depths and the subsidence behavior of hotspot volcanoes [*Turner et al.*, 1980; *Lonsdale*, 1988; *McNutt et al.*, 1990; *Van Waasbergen and Winterer*, 1993]. Recent research, however, suggests that some intraplate volcanism may not be due to hotspots and, instead, may result from stresses within the lithosphere [*Sandwell et al.*, 1995; *McNutt et al.*, 1997], small-scale convection [*King and Anderson*, 1995], or compositional anomalies in the mantle [*Bonatti*, 1990]. Because a thermal anomaly such as a hotspot results in uplift of the regional seafloor, anomalously shallow seafloor depths should be preserved in the heights of hotspot volcanoes.

The primary goal of this study is to use guyot heights to determine oceanic paleodepth. In so doing we can determine whether or not the volcanoes in this study formed over hotspots and, if so, quantify thermal anomalies associated with the observed uplift. Additionally, we can use these data to investigate height variations within individual volcanic chains. Because seafloor depth increases with age, we expect guyots formed on older seafloor to be taller than those formed on young seafloor. We therefore examine guyot heights as a function of the age contrast between the volcano and the underlying lithosphere. In addition, whereas other researchers have considered the height of the guyot as extending to the top of the reef or sediment, in this paper we measure the height to the slope break of the volcanic basement, which is our best estimate for the seafloor depth at the time of volcanism.

In this paper we compile previously published data on 114 intraplate volcanoes that are either currently subaerial or have been subaerial at one time (Figure 1). These data are displayed in Figure 2 where it is shown that the heights of nearly all of the guyots, atolls, and islands examined in this study are anomalously low, given the age of the seafloor on which they formed. We then compare observed guyot heights with new thermal models in which the lithosphere is underlain by anomalously hot mantle. Later, we focus on individual volcanic groups and discuss possible causes of height variation within each group. Finally, we investigate the Hawaiian-Emperor chain as a special case where a single hotspot has formed volcanoes on lithosphere with a large range of ages. These studies suggest that Meiji guyot, assumed to be the oldest and northernmost of the Emperor seamounts, probably formed near a spreading center.

2. Data

Tables 1 and 2 list age and height data for the 114 volcanoes included in this study as compiled from a number of sources. In selecting volcanoes to study it is important to differentiate between those seamounts that have eroded flat and those that simply have a guyot-like morphology [*Simkin*, 1972]. For example, *Smoot* [1985] argues that the flat top of Daikakuji guyot in the Hawaiian chain may be the result of a slumped caldera rather than

Paper number 1999JB900386.
0148-0227/00/1999JB900386$09.00

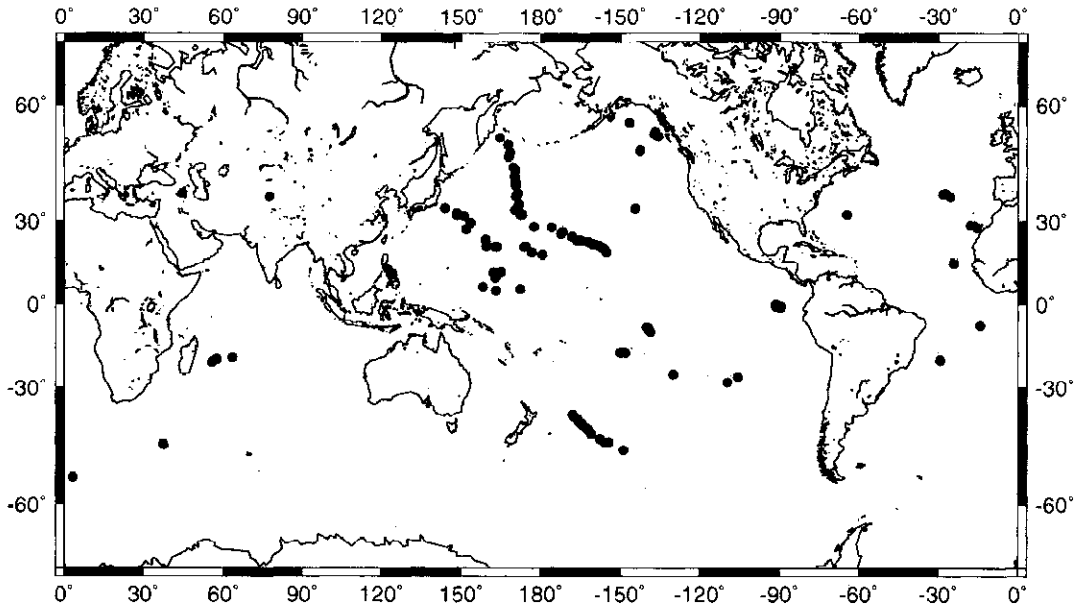

Figure 1. Locations of the guyots, atolls, and islands used in this study (precise locations given in Table 1).

an eroded flat top. Recent high-resolution hydrosweep mapping, however, shows no indication of a slumped caldera [*Weinrebe et al.*, 1997], and thus we include Daikakuji in this study. In general, guyots were selected for this study only if evidence exists that they were once subaerial or if they are currently subaerial (atolls or islands). The presence of shallow water or subaerially deposited sediments such as shallow reef carbonates or gravel were confirmed on all of the guyots in this study that have been drilled or dredged.

Our goal is to relate seafloor paleodepths, as inferred from guyot heights, to the age of the seafloor as near to the time of volcanism as possible. To ascertain the heights of guyots as a function of age, we need four primary pieces of data: the current depth to basement of the regional seafloor near a guyot, the depth of the guyot's slope break, and the ages of guyot and seafloor.

Caution must be taken in defining regional seafloor depth, as many of the guyots presented in this study are surrounded by moats produced by lithospheric flexure. In addition, the proxim-

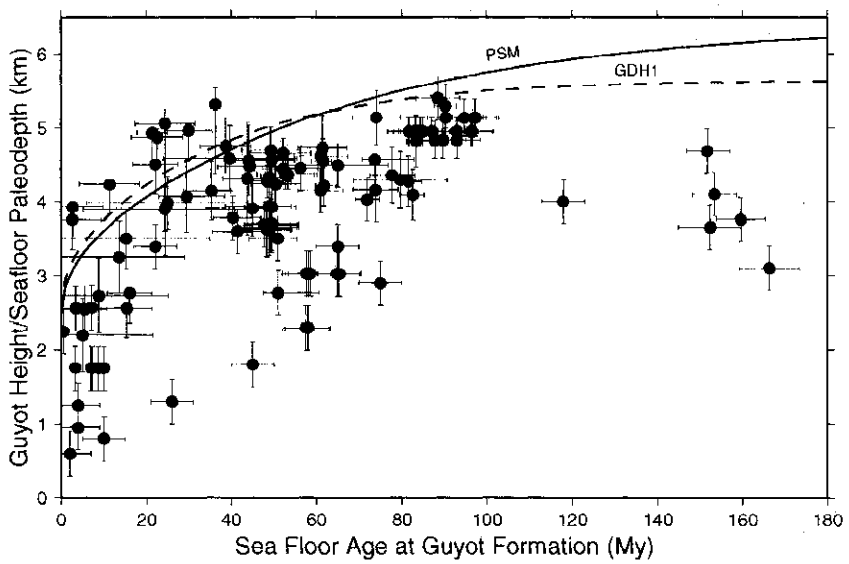

Figure 2. Guyot height plotted against sea floor age at the time the guyot formed. Curves show height predicted if the seamounts eroded flat at sea level and stood on normal seafloor, according to the models of *Parsons and Sclater* [1977] (solid curve) and *Stein and Stein* [1992] (dashed curve). Heights of nearly all volcanoes in this study are significantly lower than predicted by normal age-depth curves. Data for Figure 2 are shown in Table 1. Height error bars are calculated by summing uncertainties in the location of guyot slope break, regional seafloor depth, and seafloor sediment thickness. Age error bars are the sum of uncertainties in volcano and seafloor ages.

Table 1. Volcano Age and Depth Data

Volcano	Volcano Age, Myr	Age Unc., Myr	Dating Method	Max. Height of Guyot, m	Depth to Slope Break, m	Sed. Thick., m	Depth to Basement	Drilled Depth to Basement, m	Isostatic Corr., m	Depth Uncert., m	Hotspot	Ocean	Volcano Longitude	Volcano Latitude
Meiji	85.0	8.5	interp.	3015	-	1044	4059	4059	454	100	HE	PAC	164.5 E	53.2 N
Detroit	81.2	1.3	Ar-Ar	2385	-	856	3241	3241	372	100	HE	PAC	167.6 E	51.5 N
Suizei	76.4	3.8	interp.	2015	3000	800	3000	-	348	185	HE	PAC	168.2 E	49.7 N
Tenji	74.8	3.7	interp.	1630	2500	-	2500	-	0	100	HE	PAC	167.8 E	48.7 N
Jimmu	70.7	3.5	interp.	1250	2000	-	2000	-	0	100	HE	PAC	169.5 E	46 N
North Suiko	68.5	3.4	interp.	1325	1830	225	1830	-	0	280	HE	PAC	170 E	45.8 N
Suiko	64.7	1.1	Ar-Ar	1094	1823	164	1823	2025	71	202	HE	PAC	170.3 E	45 N
Soga	64.6	3.2	interp.	1276	1823	-	1823	-	0	100	HE	PAC	170 E	43.4 N
Showa	63.5	3.2	interp.	1458	2005	-	2005	-	0	100	HE	PAC	170.33 E	43 N
Yomei	62.2	3.1	interp.	911	2005	200	2005	1904	87	101	HE	PAC	170.33 E	42.33 N
Ninigi	61.0	3.1	interp.	1280	2100	-	2100	-	0	100	HE	PAC	170.25 E	41.75 N
Godaigo	61.0	3.1	interp.	1650	2830	-	2830	-	0	100	HE	PAC	170.5 E	41.8 N
Nintoku	56.7	0.6	Ar-Ar	1094	1276	74	1276	1384	32	108	HE	PAC	170.5 E	41 N
Jingu	55.4	0.9	Ar-Ar	911	1094	-	1094	-	0	100	HE	PAC	171.2 E	38.7 N
Ojin	55.2	0.7	Ar-Ar	1094	1458	59	1458	1538	26	80	HE	PAC	170.5 E	38 N
Koko	48.1	0.8	K-Ar	337	1605	200	1605	-	87	100	HE	PAC	171.75 E	35.5 N
Kimmei	39.9	1.2	K-Ar	-	1098	-	1098	-	0	100	HE	PAC	170.33 E	33.75 N
Yuryaku	43.4	1.6	K-Ar	547	1276	-	1276	-	0	100	HE	PAC	172.33 E	32.67 N
Daikakuji	42.4	2.3	K-Ar	1094	1458	-	1458	-	0	100	HE	PAC	172.25 E	32.08 N
Kammu	41.6	2.1	interp.	365	729	-	729	-	0	100	HE	PAC	173 E	32.25 N
Midway	27.7	0.6	K-Ar	0	0	364	0	-	158	50	HE	PAC	177.4 E	28.2 N
Pearl and Hermes Reef	20.6	0.5	K-Ar	0	0	200	0	-	87	50	HE	PAC	175.9 W	28 N
Northampton	26.6	2.7	K-Ar	0	0	200	0	-	87	50	HE	PAC	172.3 W	25.8 N
Laysan	19.9	0.3	K-Ar	0	0	200	0	-	87	50	HE	PAC	171.8 W	26.5 N
Gardner	12.3	1.0	K-Ar	0	0	200	0	-	87	50	HE	PAC	168.1 W	24.8 N
La Perouse Pinnacles	12.0	0.4	K-Ar	0	0	200	0	-	87	50	HE	PAC	166.4 W	23.5 N
Necker	10.3	0.4	K-Ar	0	0	200	0	-	87	50	HE	PAC	164.8 W	23.4 N
Nihoa	7.2	0.3	K-Ar	0	0	200	0	-	87	50	HE	PAC	162.1 W	23 N
Niihau	4.9	0.1	K-Ar	0	0	0	0	-	0	0	HE	PAC	160.2 W	22 N
Waianae	3.7	0.1	K-Ar	0	0	0	0	-	0	0	HE	PAC	158.2 W	21.6 N

Table 1. (continued)

Volcano	Volcano Age, Myr	Age Unc., Myr	Dating Method	Max. Height of Guyot, m	Depth to Slope Break, m	Sed. Thick., m	Depth to Basement	Drilled Depth to Basement, m	Isostatic Corr., m	Depth Uncert., m	Hotspot	Ocean	Volcano Longitude	Volcano Latitude
Koolau	2.6	0.1	K-Ar	0	0	0	0	-	0	0	HE	PAC	158 W	21.6 N
West Molokai	1.9	0.1	K-Ar	0	0	0	0	-	0	0	HE	PAC	157.2 W	21.1 N
Lanai	1.3	0.0	K-Ar	0	0	0	0	-	0	0	HE	PAC	157 W	20.9 N
East Maui	0.8	0.0	K-Ar	0	0	0	0	-	0	0	HE	PAC	156.2 W	20.6 N
Kohala	0.4	0.0	K-Ar	0	0	0	0	-	0	0	HE	PAC	155.7 W	20 N
Kilauea	0.0	0.0	K-Ar	0	0	0	0	-	0	0	HE	PAC	155.3 W	19.3 N
Kusaie	1.3	0.2	-	0	0	0	0	-	0	0	CAR	PAC	163 E	5.3 N
Ponape	5.4	0.8	-	0	0	0	0	-	0	0	CAR	PAC	158.15 E	6.7 N
Easter	2.5	0.4	-	0	0	0	0	-	0	0	EAS	PAC	109.6 W	28.2 S
Sala y Gomez	1.9	0.3	-	0	0	0	0	-	0	0	EAS	PAC	105.7 W	26.4 S
Wolf	0.7	0.1	-	0	0	0	0	-	0	0	GAL	PAC	91.25 W	0
Santa Cruz	1.0	0.2	-	0	0	0	0	-	0	0	GAL	PAC	90.33 W	0.6 S
San Cristobal	0.7	0.1	-	0	0	0	0	-	0	0	GAL	PAC	89.5 W	0.8 S
Espanola	3.3	0.5	-	0	0	0	0	-	0	0	GAL	PAC	89.67 W	1.42 S
Isabela	0.0	0.0	-	0	0	0	0	-	0	0	GAL	PAC	91.17 W	0.92 S
Takuyo Daisan (Seiko)	118.4	1.8	Ar-Ar	1501	1550	191	1550	1692	83	142	JPN	PAC	144.3 W	34.2 N
MIT	120.3	0.8	Ar-Ar	1280	1400	728	1400	2050	316	650	JPN	PAC	151.83 E	27.28 N
Takuyo Daini	118.5	1.1	Ar-Ar	1420	1510	200	1510	1620	87	110	JPN	PAC	143.87 E	34.3 N
Johnson	108.3	10.8	Ar-Ar	1460	1800	200	1800	1660	87	140	JPN	PAC	148.25 E	31.98 N
Winterer	108.3	1.0	Ar-Ar	1360	1630	200	1630	1560	87	70	JPN	PAC	148.32 E	32.78 N
Isakov	103.7	1.8	Ar-Ar	1380	1590	200	1590	1580	87	10	JPN	PAC	151.17 E	31.57 N
Makarov	93.9	1.3	Ar-Ar	1340	1420	200	1420	1540	87	120	JPN	PAC	153.48 E	29.47 N
148.8W	12.5	0.4	Ar-Ar	-	530	-	530	-	0	50	LOU	PAC	148.8 W	48.2 S
154.3W	17.2	1.7	interp.	-	630	-	630	-	0	50	LOU	PAC	154.3 W	46.1 S
155.9W	18.7	1.9	interp.	-	630	-	630	-	0	50	LOU	PAC	155.9 W	46.2 S
157.6W	18.0	5.0	Ar-Ar	-	720	-	720	-	0	50	LOU	PAC	157.6 W	45.4 S
160.7W	24.6	2.5	interp.	-	820	-	820	-	0	50	LOU	PAC	160.7 W	44 S
162W	27.8	2.8	interp.	-	850	-	850	-	0	50	LOU	PAC	162 W	42.8 S
162.8W	29.8	3.0	interp.	-	740	-	740	-	0	50	LOU	PAC	162.8 W	42.3 S
164.3W	35.5	0.6	Ar-Ar	-	1125	-	1125	-	0	75	LOU	PAC	164.3 W	41.5 S

Table 1. (continued)

Volcano	Volcano Age, Myr	Age Unc., Myr	Dating Method	Max. Height of Guyot, m	Depth to Slope Break, m	Sed. Thick., m	Depth to Basement	Drilled Depth to Basement, m	Isostatic Corr., m	Depth Uncert., m	Hotspot	Ocean	Volcano Longitude	Volcano Latitude
165W	34.6	3.5	interp.	-	960	-	960	-	0	50	LOU	PAC	165 W	40.9 S
165.4W	35.4	3.5	interp.	-	1225	-	1225	-	0	75	LOU	PAC	165.4 W	40.7 S
165.7W	36.6	3.7	interp.	-	1470	-	1470	-	0	50	LOU	PAC	165.7 W	40.4 S
166.1W	37.8	3.8	interp.	-	1500	-	1500	-	0	50	LOU	PAC	166.1 W	39.9 S
166.3W	38.0	3.8	interp.	-	1530	-	1530	-	0	50	LOU	PAC	166.3 W	39.7 S
166.6W	38.6	3.9	interp.	-	1525	-	1525	-	0	75	LOU	PAC	166.6 W	39.6 S
167.4W	40.0	4.0	interp.	-	1265	-	1265	-	0	75	LOU	PAC	167.4 W	39.1 S
168W	45.0	0.5	Ar-Ar	-	1245	-	1245	-	0	75	LOU	PAC	168 W	38.4 S
Lo-En	112.8	1.2	Ar-Ar	1084	1400	140	1400	1224	61	176	MAR	PAC	162.8 E	10.2 N
Wodejebato	83.2	1.1	Ar-Ar	1334	1400	175	1400	1509	76	109	MAR	PAC	164.9 E	12 N
Limalok	69.5	5.0	Ar-Ar	1265	1800	451	1800	1716	196	84	MAR	PAC	172.33 E	5.7 N
Anawetok	75.9	0.6	Ar-Ar	0	-	1347	1347	1347	585	64	MAR	PAC	162.16 E	11.92 N
Allison	101.2	0.8	Ar-Ar	1300	1900	840	1900	2360	365	460	MID	PAC	179.5 W	18.5 N
Heezen	123.1	0.6	Ar-Ar	1240	1290	920	1290	-	400	100	MID	PAC	173.8 E	21.2 N
Jacqueline	98.5	1.4	Ar-Ar	1540	1750	690	1750	-	300	100	MID	PAC	176.7 E	19.3 N
Resolution	127.6	2.1	Ar-Ar	1300	1500	1620	1500	2982	704	1482	MID	PAC	174.3 E	21.3 N
Hiva Oa	2.6	0.4	-	0	0	0	0	0	0	0	MRQ	PAC	139 W	9.75 S
Nuku Hiva	4.3	0.7	-	0	0	0	0	0	0	0	MRQ	PAC	140.15 W	8.87 S
Tahuatu	2.1	0.3	-	0	0	0	0	0	0	0	MRQ	PAC	139.1 W	10 S
Mohotani	1.9	0.3	-	0	0	0	0	0	0	0	MRQ	PAC	138.9 W	10 S
Ua Huka	2.8	0.4	-	0	0	0	0	0	0	0	MRQ	PAC	139.53 W	8.92 S
Fatu Hiva	1.4	0.2	-	0	0	0	0	0	0	0	MRQ	PAC	138.7 W	10.5 S
Pitcairn	1.0	0.1	-	0	0	0	0	0	0	0	PIT	PAC	130 W	25.5 S
Mehetia	0.0	0.0	-	0	0	0	0	0	0	0	SOC	PAC	148.07 W	17.87 S
Tahiti	1.0	0.2	-	0	0	0	0	0	0	0	SOC	PAC	149.5 W	17.67 S
Tahiti-iti	0.6	0.1	-	0	0	0	0	0	0	0	SOC	PAC	149.2 W	17.8 S
Moorea	2.1	0.3	-	0	0	0	0	0	0	0	SOC	PAC	150 W	17.8 S
Wilde	90.6	0.3	Ar-Ar	1300	1440	0	1440	1300	0	140	WAK	PAC	163.3 E	21.17 N
Scripps	101.6	0.7	Ar-Ar	1260	1420	0	1420	1260	0	140	WAK	PAC	159.33 E	23.78 N
Vibelius	139.0	14.0	magnetics	1840	2040	400	2040	2240	174	60	WAK	PAC	162.77 E	21.22 N

Table 1. (continued)

Volcano	Volcano Age, Myr	Age Unc., Myr	Dating Method	Max. Height of Guyot, m	Depth to Slope Break, m	Sed. Thick., m	Depth to Basement	Drilled Depth to Basement, m	Isostatic Corr., m	Depth Uncert., m	Hotspot	Ocean	Volcano Longitude	Volcano Latitude
Lamont	87.2	0.3	Ar-Ar	1260	1340	0	1340	1260	0	80	WAK	PAC	159.5 E	21.52 N
Denson	18.2	2.0	K-Ar	922	-	-	922	-	0	100	PW	PAC	137.4 W	54 N
Horton	20.7	2.0	K-Ar	761	-	-	761	-	0	100	PW	PAC	142.6 W	50.3 N
Bowie	0.7	1.0	K-Ar	235	-	-	235	-	0	100	PW	PAC	135.6 W	53.5 N
Dickins	4.0	0.2	K-Ar	474	-	-	474	-	0	100	PW	PAC	136.9 W	54.6 N
Giacomini	20.9	0.4	K-Ar	636	-	100	636	736	43	100	PW	PAC	146.6 W	56.5 N
Davidson	17.4	1.7	K-Ar	1249	-	-	1249	-	0	100	PW	PAC	136.5 W	53.7 N
Ascension	1.5	0.2	-	0	0	0	0	0	0	0	ASC	ATL	14.23 W	7.95 S
Ilha do Pico	0.0	0.0	-	0	0	0	0	0	0	0	AZO	ATL	28.3 W	38.5 N
Terceira	0.0	0.0	-	0	0	0	0	0	0	0	AZO	ATL	27.2 W	38.7 N
Sao Miguel	0.0	0.0	-	0	0	0	0	0	0	0	AZO	ATL	25.5 W	37.8 N
Bermuda	45.0	6.8	-	0	0	0	0	0	0	0	BER	ATL	64.5 W	32.2 N
Bouvet	0.0	0.0	-	0	0	0	0	0	0	0	BOU	ATL	3.4 E	54.43 S
Tenerife	15.7	2.4	-	0	0	0	0	0	0	0	CAN	ATL	16.5 W	28.5 N
La Palma	1.6	0.2	-	0	0	0	0	0	0	0	CAN	ATL	17.8 W	28.8 N
Gran Canaria	13.7	2.1	-	0	0	0	0	0	0	0	CAN	ATL	15.6 W	28 N
Fogo	0.0	0.0	-	0	0	0	0	0	0	0	CVR	ATL	24.2 W	15.2 N
Trindade	1.5	0.2	-	0	0	0	0	0	0	0	TRN	ATL	29.3 W	20.5 S
Amsterdam	0.0	0.0	-	0	0	0	0	0	0	0	AMP	IND	77.5 E	37.8 N
St. Paul	0.0	0.0	-	0	0	0	0	0	0	0	AMP	IND	44.5 E	38.7 N
Prince Edward	0.0	0.0	-	0	0	0	0	0	0	0	PE	IND	37.5 E	46.5 S
Marion	0.0	0.0	-	0	0	0	0	0	0	0	PE	IND	37.5 E	46.8 S
Rodrigues	1.6	0.2	-	0	0	0	0	0	0	0	REU	IND	63.4 E	19.7 S
Mauritius	7.8	1.2	-	0	0	0	0	0	0	0	REU	IND	57.5 E	20.25 S
Reunion	2.0	0.3	-	0	0	0	0	0	0	0	REU	IND	55.7 E	21.2 S

References for each volcano are included in Table 2. Hotspots and oceans are abbreviated as follows: AMP, Amsterdam-St. Paul; ASC, Ascension; ATL, Atlantic Ocean; AZO, Azores; BER, Bermuda; BOU, Bouvet; CAN, Canary Islands; CAR, Caroline; CVR, Cape Verde; EAS, Easter; GAS, Galapagos; HE, Hawaiian-Emperor; IND, Indian Ocean; JPN, Japanese or Geisha seamounts; LOU, Louisville; MAR, Marshall Islands; MID, Mid-Pacific mountains; MRQ, Marquesas; PAC, Pacific Ocean; PE, Prince Edward; PIT, Pitcairn; PW, Pratt-Welker; REU, Reunion; SOC, Society Islands; TRN, Trindade; WAK, Wake seamounts). Other abbreviations are unc., uncertainty; max., maximum; sed. thick., sediment thickness; corr., correction; interp., interpolated.

Table 2. Seafloor Age and Depth Data

Volcano	Seafloor Age, Myr	Seafloor Age Uncert., Myr	Seafloor Depth, m	Depth Uncert., m	Sed. Thick., m	Sed. Uncert., m	Age at Guyot Formation,* Myr	Age Uncert.,* Myr	Guyot Height,* m	Height Uncert.,* m	References
Meiji	90	15	5300	300	500	100	5.0	23.5	2195	500	1, 2, 3
Detroit	90	15	5300	300	300	100	8.8	16.3	2731	500	2, 4, 5
Suizei	90	15	5600	200	300	100	13.6	18.8	3248	485	2, 5
Tenji	90	15	5700	200	300	100	15.2	18.7	3500	400	2, 5
Jimmu	95	15	5700	100	200	100	24.3	18.5	3900	300	2, 6
North Suiko	98	5	5700	100	200	100	29.5	8.4	4070	480	2, 6, 7, 8, 9
Suiko	100	5	5700	100	200	100	35.3	6.1	4148	402	2, 6, 7, 8, 9
Soga	105	5	5400	100	200	100	40.4	8.2	3777	300	2, 6, 7, 8, 9
Showa	105	5	5400	100	200	100	41.5	8.2	3595	300	2, 6, 7, 8, 9
Yomei	110	5	5400	100	200	100	47.8	8.1	3682	301	2, 6, 7, 8, 9
Ninigi	112	5	5400	100	200	100	51.0	8.1	3500	300	2, 9, 10
Godaigo	112	5	5400	100	200	100	51.0	8.1	2770	300	2, 9, 10
Nintoku	113	5	5500	100	200	100	56.3	5.6	4456	308	2, 6, 8, 9
Jingu	117	2	5450	100	200	100	61.6	2.9	4556	300	2, 6, 8, 9
Ojin	117	2	5450	100	200	100	61.8	2.7	4218	280	2, 6, 8, 9
Koko	120	2	5350	100	200	100	71.9	2.8	4032	300	2, 8, 9, 11
Kimmei	125	2	5600	100	200	100	85.1	3.2	4702	300	2, 9, 12
Yuryaku	125	2	5350	150	200	100	81.6	3.6	4274	350	2, 9, 12
Daikakuji	125	2	5350	150	200	100	82.6	4.3	4092	350	2, 9, 12
Kammu	125	2	5350	150	200	100	83.4	4.1	4821	350	2, 9, 12
Midway	118	2	5350	150	150	100	90.3	2.6	5658	300	2, 9, 13
Pearl and Hermes Reef	118	5	5100	100	150	100	97.4	5.5	5337	250	2, 9
Northampton	117	5	5100	100	150	100	90.4	7.7	5337	250	2, 9
Laysan	117	5	5100	100	150	100	97.1	5.3	5337	250	2, 9
Gardner	107	5	5100	100	150	100	94.7	6.0	5337	250	2, 9
La Perouse Pinnacles	105	5	4800	100	150	100	93.0	5.4	5037	250	2, 9
Necker	100	5	4800	100	150	100	89.7	5.4	5037	250	2, 9
Nihoa	95	5	4800	100	150	100	87.8	5.3	5037	250	2, 9
Niihau	92	5	4800	100	150	100	87.1	5.1	4950	200	2, 9
Kauai	90	5	4800	100	150	100	84.9	5.2	4950	200	2, 9

Table 2. (continued)

Volcano	Seafloor Age, Myr	Seafloor Age Uncert., Myr	Seafloor Depth, m	Depth Uncert., m	Sed. Thick., m	Sed. Uncert., m	Age at Guyot Formation,* Myr	Age Uncert.,* Myr	Guyot Height,* m	Height Uncert.,* m	References
Waianae	87	5	4800	100	150	100	83.3	5.1	4950	200	2, 9
Koolau	87	5	4800	100	150	100	84.4	5.1	4950	200	2, 9
West Molokai	85	5	4800	100	150	100	83.1	5.1	4950	200	2, 9
Lanai	83	5	4800	100	150	100	81.7	5.0	4950	200	2, 9
East Maui	97	5	4800	100	150	100	96.3	5.0	4950	200	2, 9
Kohala	97	5	4800	100	150	100	96.6	5.0	4950	200	2, 9
Kilauea	93	5	4800	100	150	100	93.0	5.0	4950	200	2, 9
Kusaie	153	5	4389	200	300	100	151.7	5.2	4689	300	14
Ponape	165	5	3658	200	100	100	159.6	5.8	3758	300	14
Easter	3	1	2200	200	50	100	0.5	1.4	2250	300	14
Sala y Gomez	9	1	2520	200	50	100	7.1	1.3	2570	300	14
Wolf	4	1	1000	200	750	100	3.3	1.1	1750	300	14
Santa Cruz	8	1	1000	200	750	100	7.0	1.2	1750	300	14
San Cristobal	8	1	1000	200	750	100	7.3	1.1	1750	300	14
Espanola	12	1	1000	200	750	100	8.7	1.5	1750	300	14
Isabela	10	1	1000	200	750	100	10.0	1.0	1750	300	14
Takuyo Daisan (Seiko)	139.7	1.75	5700	250	700	100	21.3	3.6	4933	492	8, 15, 16, 17, 18
MIT	156.6	0.6	5900	250	500	100	36.3	1.4	5316	1000	8, 15, 16, 17, 18, 19
Takuyo Daini	141	5	5600	250	700	100	22.5	6.1	4877	460	8, 15, 16, 17
Johnson	148	5	5900	250	400	100	39.7	15.8	4587	490	8, 17
Winterer	147	5	5900	250	400	100	38.7	6.0	4757	420	8, 17, 19
Isakov	153	5	5900	250	300	100	49.3	6.8	4697	360	8, 17, 19
Makarov	155	5	5651	250	300	100	61.1	6.3	4618	470	8, 17, 20
148.8W	62	5	5000	100	100	50	49.5	5.4	4570	200	9, 21
154.3W	70	5	4900	100	100	50	52.8	6.7	4370	200	9, 21
155.9W	72	5	4900	100	100	50	53.3	6.9	4370	200	9, 21
157.6W	67	5	4950	100	100	50	49.0	10.0	4330	200	9, 21
160.7W	69	5	5200	100	100	50	44.4	7.5	4480	200	9, 21
162W	80	5	5200	100	100	50	52.2	7.8	4450	200	9, 21
162.8W	82	5	5200	100	200	50	52.2	8.0	4660	200	9, 21

Table 2. (continued)

Volcano	Seafloor Age, Myr	Seafloor Age Uncert., Myr	Seafloor Depth, m	Depth Uncert., m	Sed. Thick., m	Sed. Uncert., m	Age at Guyot Formation,* Myr	Age Uncert.,* Myr	Guyot Height,* m	Height Uncert.,* m	References
164.3W	84	5	5200	100	200	50	48.5	5.6	4275	225	9, 21
165W	85	5	4950	250	250	50	50.4	8.5	4240	350	9, 21
165.4W	85	5	4950	250	200	50	49.6	8.5	3925	375	9, 21
165.7W	86	5	4950	250	200	50	49.4	8.7	3680	350	9, 21
166.1W	87	5	4950	250	200	50	49.2	8.8	3650	350	9, 21
166.3W	87	5	4950	250	200	50	49.0	8.8	3620	350	9, 21
166.6W	87	5	4950	250	200	50	48.4	8.9	3625	375	9, 21
167.4W	89	5	4950	250	250	50	49.0	9.0	3935	375	9, 21
168W	90	5	4950	250	200	50	45.0	5.5	3905	375	9, 21
Lo-En	156.9	5	5200	250	700	100	44.1	6.2	4561	526	17, 18, 22
Wodejebato	156.9	5	5200	250	700	100	73.7	6.1	4576	459	17, 18, 22
Limalok	149.2	6	5200	250	700	100	79.7	11.0	4296	434	17, 18, 22
Anawetok	150	5	5200	200	700	100	74.1	5.6	5139	364	17, 18, 22
Allison	145	5	5500	250	350	100	43.8	5.8	4315	810	17, 19, 23, 24
Heezen	153	5	5500	200	350	100	29.9	5.6	4960	400	17, 19
Jacqueline	148	5	4800	200	350	100	49.5	6.4	3700	400	17, 19, 24
Resolution	152	5	5500	200	350	100	24.4	7.1	5054	1782	17, 18, 23
Hiva Oa	60	5	2195	200	100	100	57.5	5.4	2295	300	14
Nuku Hiva	62	5	2926	200	100	100	57.7	5.7	3026	300	14
Tahuatu	60	5	2195	200	100	100	57.9	5.3	2295	300	14
Mohotani	60	5	2195	200	100	100	58.1	5.3	2295	300	14
Ua Huka	61	5	2926	200	100	100	58.2	5.4	3026	300	14
Fatu Hiva	60	5	2926	200	100	100	58.6	5.2	3026	300	14
Pitcairn	23	5	3292	200	100	100	22.1	5.1	3392	300	14
Mehetia	65	5	3292	200	100	100	65.0	5.0	3392	300	14
Tahiti	66	5	2926	200	100	100	65.0	5.2	3026	300	14
Tahiti-iti	66	5	2926	200	100	100	65.4	5.1	3026	300	14
Moorea	67	5	2926	200	100	100	64.9	5.3	3026	300	14
Wilde	164.5	5	5250	200	350	100	73.9	5.3	4160	440	15, 17
Scripps	163	5	5800	200	350	100	61.4	5.7	4730	440	15, 17

Table 2. (continued)

Volcano	Seafloor Age, Myr	Seafloor Age Uncert., Myr	Seafloor Depth, m	Depth Uncert., m	Sed. Thick., m	Sed. Uncert., m	Age at Guyot Formation,* Myr	Age Uncert.,* Myr	Guyot Height,* m	Height Uncert.,* m	References
Vibelius	164	5	5500	200	350	100	25.0	19.0	3984	360	15, 17
Lamont	165	5	5350	200	350	100	77.8	5.3	4360	380	15, 17
Denson	21	5	4500	200	350	100	2.8	7.0	3928	400	25, 26
Horton	32	5	4500	200	500	100	11.3	7.0	4239	400	25, 26
Bowie	16	5	2195	200	600	100	15.3	6.0	2560	400	25, 26
Dickins	20	5	2560	200	680	100	16.0	5.2	2766	400	25, 26
Giacomini	43	5	4500	200	600	100	22.1	5.4	4507	400	25, 26
Davidson	20	5	4500	200	500	100	2.6	6.7	3751	400	25, 26
Ascension	7	5	2500	200	50	100	5.5	5.2	2550	300	14
Ilha do Pico	10	5	500	200	300	100	10.0	5.0	800	300	14
Terceira	26	5	1000	200	300	100	26.0	5.0	1300	300	14
Sao Miguel	45	5	1500	200	300	100	45.0	5.0	1800	300	14
Bermuda	110	5	4000	200	500	100	65.0	11.8	4500	300	14
Bouvet	2	5	500	200	100	100	2.0	5.0	600	300	14
Tenerife	168	5	2500	200	1150	100	152.3	7.4	3650	300	14
La Palma	155	5	3000	200	1100	100	153.4	5.2	4100	300	14
Gran Canaria	180	5	2000	200	1100	100	166.3	7.1	3100	300	14
Fogo	118	5	3000	200	1000	100	118.0	5.0	4000	300	14
Trindade	90	5	4900	200	500	100	88.5	5.2	5400	300	14
Amsterdam	4	5	1200	200	49	100	4.0	5.0	1249	300	14
St. Paul	4	5	900	200	51	100	4.0	5.0	951	300	14
Prince Edward	75	5	2500	200	400	100	75.0	5.0	2900	300	14
Marion	75	5	2500	200	400	100	75.0	5.0	2900	300	14
Rodrigues	5	5	2500	200	55	100	3.4	5.2	2555	300	14
Mauritius	57	5	3500	200	150	100	49.2	6.2	3650	300	14
Reunion	63	5	4000	200	150	100	61.0	5.3	4150	300	14

Abbreviations are the same as given in Table 1. References: 1, *Scholl and Creager* [1973]; 2, *Clague* [1996]; 3, *Scholl et al.* [1977]; 4, *Keller et al.* [1995]; 5, *Lonsdale et al.* [1993]; 6, *Clague et al.* [1980]; 7, *Smoot* [1982]; 8, *Vogt and Smoot* [1984]; 9, *Muller et al.* [1997]; 10, *Smoot* [1983]; 11, *Davies et al.* [1972]; 12, *Smoot* [1985]; 13, *Ladd et al.* [1967]; 14, *Epp* [1984]; 15, *Premoli Silva et al.* [1993]; 16, *Haggerty and Premoli Silva* [1995]; 17, *Van Waasbergen and Winterer* [1993]; 18, *Pringle and Duncan* [1995]; 19, *Winterer and Sager* [1993]; 20, *McNutt et al.* [1990]; 21, *Lonsdale* [1988]; 22, *Bergersen* [1995]; 23, *Sager et al.* [1993]; 24, *Pringle and Duncan* [1993]; 25, *Turner et al.* [1980]; 26, *Winterer* [1989].

*The data in these columns are plotted in Figures 2, 5, 6, and 8.

ity of other volcanoes can complicate estimates of seafloor depth surrounding a volcano. To minimize these effects, we define regional seafloor depth to lie beyond the flexural moat and at a distance from neighboring volcanoes. Seafloor depths were either estimated from ETOPO5 data or previous studies (see Table 2). We approximate a measurement error of ~100-300 m for seafloor depth. To best estimate the paleodepth when the guyot formed, we consider the depth of volcanic basement beneath the seafloor sediments. We used sediment thickness data from published studies (Table 2) or from sediment thickness maps [*Ludwig and Houtz*, 1979; *Winterer*, 1989]. The values for sediment thickness were then added to seafloor depths to obtain seafloor basement depths. We note that this measurement may have the effect of overestimating guyot heights, since the volcano may have formed on previously sedimented seafloor.

To determine a guyot's height, we calculate the difference between the current basement depth of regional seafloor and the depth to significant slope break on the guyot. We chose slope break rather than maximum elevation because postsubmergence volcanics, sediment, coral caps, and rapid subsidence may record sea level later in the volcano's history and may result in a guyot's having significant summit topography. Even volcanic islands show a dramatic difference between the steep slopes of the submarine portion of the edifice and the relatively flatter subaerial slopes. We therefore believe that slope break records sea level at the time of erosion and that it represents the best available estimate of sea level at the time of volcanism. We estimated the location of slope break from published figures where high-resolution bathymetric data or seismic reflection profiles were available; otherwise, we used previously published values (see Table 1). Because tilting of the volcanic edifice may result in >300 m variation in the location of the main slope break [*Lonsdale*, 1988; *Van Waasbergen and Winterer*, 1993], we selected an average depth and incorporated the range into our uncertainties. The depth to slope break is estimated for all volcanoes in this study except those in the Pratt-Welker chain where only the maximum height is known. For currently subaerial volcanoes we measure the surrounding regional seafloor depth directly and ignore their subaerial heights.

The thickness of pelagic sediment or carbonate accumulated over the top of the eroded edifice is a source of height measurement uncertainty. As an atoll ages, its carbonate reef often grows vertically, maintaining the height of the seamount at sea level, even as the edifice subsides. The presence of this reef may mask the location of the slope break of the guyot's volcanic basement, an effect which cannot be measured without drilling or seismic reflection data. Lo-En guyot in the Marshall Islands is shown in Figure 3, exemplifying the case where a seismic reflection profile is required to accurately determine the position of volcanic slope break. Where such data are unavailable, the presence of reef or pelagic sediment would cause us to overestimate the height of the guyot, sometimes significantly. In such cases, we can consider other indicators of the depth to volcanic basement. On volcanoes that have been drilled, the depth to volcanic basement is precisely measured for at least one point on the guyot's top. However, many guyots exhibit hundreds of meters of volcanic topography [*Vogt and Smoot*, 1984; *Van Waasbergen and Winterer*, 1993], making it possible that the depth to basement inferred from drilling does not accurately represent the position of flat top erosion. Rather than base our calculations on a single point, we rely first on estimates of slope break and incorporate depths from drilling data into the calculated uncertainty. Where available, reef or sediment thicknesses are listed in Table 1.

Calculating the age of the lithosphere during volcano formation requires constraints on the relative ages of the seamount and oceanic crust. Regional seafloor ages were determined by a variety of researchers on the basis of magnetic isochrons (Table 2). The majority of the Hawaiian-Emperor chain sits on seafloor formed during the Cretaceous normal superchron, so seafloor ages are only well constrained for the seamounts between Midway Island

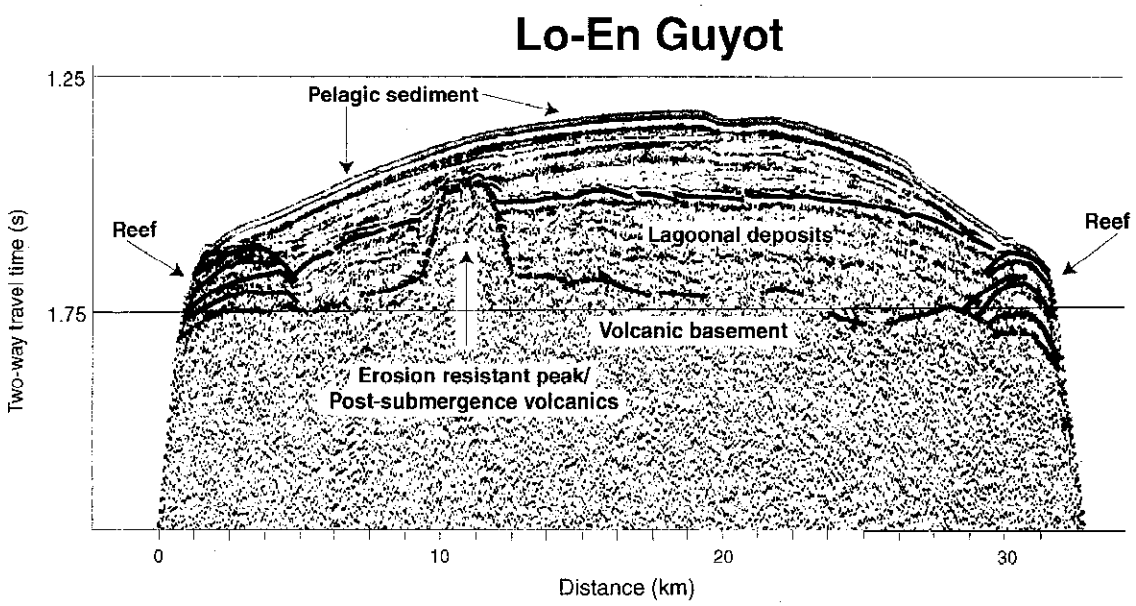

Figure 3. Single-channel seismic profile over Lo-En guyot in the Marshall Islands. Contours are pelagic sediment, reef material, lagoonal deposits, and volcanic basement. The peak shown as part of the volcanic basement is either an erosion-resistant peak or a consequence of postsubmergence volcanics and is several hundred meters in height. Each of these features must be considered when identifying the location of a guyot's flat top because each overestimates the actual guyot height.

in the Hawaiian chain and Jingu guyot in the Emperor chain (see Table 2). Seafloor ages of the Cretaceous superchron for the Hawaiian-Emperor and Louisville seamount chains were estimated using the interpolated ages of *Muller et al.* [1997]. The age of lithosphere beneath the northernmost Emperor seamounts was estimated using the plate reconstructions of *Renkin and Sclater* [1988] and *Rea and Dixon* [1983]. No seafloor age data exist for Louisville seamounts west of longitude 170°, so our analysis of the Louisville hotspot is based only on the eastern half of that chain. Seafloor age uncertainties are cited in the individual studies and range from 2-15 Myr.

Ages of the majority of volcanoes in this study were taken from published radiometric data, primarily by means of Ar-Ar or K-Ar dating methods (Table 1). In general, the ages of radiometrically dated seamounts used in this study have published errors of < 2 Myr. For those volcanoes for which age errors have not been estimated by other researchers we assume that the associated errors are between 5 and 10% of the K-Ar age and assign a 10% uncertainty [*Epp*, 1984]. We note that many of the ages cited in this study were calculated for altered rock and may therefore appear younger than their true eruption age; however, this effect is small relative to uncertainties associated with seafloor ages. We also note that most of the dated rocks were collected by dredging and are likely among the youngest rocks on the volcano. The age of Vibelius seamount in the Wake Islands was constrained using paleomagnetics [*Sager*, 1992]. The only undated seamounts used in this paper are several in the Hawaiian and Louisville chains. The ages of these volcanoes were estimated from rates and directions of hotspot Pacific plate relative motion [*Lonsdale*, 1988; *Clague*, 1996] and interpolated from radiometric dates on other volcanoes within the chain (see Table 1). For interpolated ages we assigned uncertainties of 10% in the Louisville chain and 5% for the Hawaiian-Emperor volcanoes.

3. Guyot Height and Seafloor Age at the Time of Volcanism

3.1. Results

Guyot heights are plotted in Figure 2 against the age contrast between the volcano and the underlying lithosphere. The smallest age contrasts (<25 Myr) are typically associated with those volcanoes whose heights, and thus paleo-water depths, are often < 3000 m. At greater age contrasts the guyots are typically taller, suggesting paleodepths in the range of 3000-5000 m. This general observation appears to reflect a first-order effect of lithospheric cooling.

Predicted age-depth curves for normal lithosphere [*Parsons and Sclater*, 1977; *Stein and Stein*, 1992] are included in Figure 2. The trend of increasing guyot height with age contrast is consistent with seafloor subsidence curves, but with a few exceptions, the heights of observed volcanoes are found to be lower than would be expected if they stood on normal seafloor and eroded flat at sea level. Compared to the seafloor subsidence models of either *Parsons and Sclater* [1977] or *Stein and Stein* [1992], guyot heights average >1000 m lower than predicted values. The implied seafloor depth anomalies suggest that many volcanoes record the uplift associated with the thermal swells of paleohotspots and present-day hotspots.

For any given age contrast, there is a range in guyot heights of ~2000-3000 m. While some of this height variation may reflect differences in lithospheric temperatures, we expect some scatter to reflect geologic processes such as sediment loading and flexural uplift that are unrelated to the thermal state of the underlying mantle. We discuss the importance of these effects below.

3.2. Factors Unrelated to the Thermal State of the Lithosphere

One factor that may contribute to scatter in seamount heights is the effect of reef and sediment loading, which will cause the volcano and surrounding seafloor to isostatically subside. To accurately correct for the effect of loading on the surrounding seafloor we would have to know the thickness of seafloor sediments at the time of volcanism, and these constraints are largely unavailable. Instead, to be most conservative in our height estimates, we assume that the seafloor was sediment-free at the time of volcano loading and perform isostatic corrections for all accumulated material on the summit of the volcano. Both of these corrections err to the side of height overestimation. To perform the correction, we assume Airy isostasy and an average sediment density of 2000 kg/m^3. Most seamounts in this study are not dramatically affected by isostatic correction; however, several (notably Resolution guyot, Meiji guyot, and Anawetok atoll) may have subsided by > 500 m owing to sediment loading. Because sediment thickness is not known for the Louisville chain, we were unable to perform isostatic corrections; therefore it is possible that our height calculations for these seamounts may be underestimated by < 500 m.

Among the guyots most influenced by surrounding seafloor sediment thickness are Meiji and Detroit guyots, the northernmost seamounts in the Hawaiian-Emperor chain. These guyots are located near a source of hemipelagic sediment, and hence the volcanoes and surrounding seafloor are coated in a significant (> 1000 m thick) sediment blanket known as the Meiji sediment tongue. Seismic reflection data to the north and northeast of Meiji seamount indicate that the sediment cover may be as thick as 1800 m in parts [*Scholl et al.*, 1977]. To minimize the degree to which the true seafloor depth is masked by sediment cover, we estimated Meiji's height using seafloor depths to the southwest of the guyot, in an area thought to have < 500 m of sediment [*Scholl et al.*, 1977; *Ludwig and Houtz*, 1979]. Because Meiji and Detroit likely formed on very young (< 10 Myr) lithosphere, it is probable that very little sediment existed on the crust at the time of volcano loading. In contrast, the Canary Islands in the Atlantic Ocean formed on heavily sedimented seafloor, so our assumption of zero sediment thickness results in an overprediction of volcano heights.

Another factor that contributes to height scatter in Figure 2 is the fact that radiometric dating records the age of volcanism, whereas the height of the guyot records the seafloor depth at the time the volcano eroded to sea level. These ages differ by an unknown time period, the time required to erode the subaerial portion of the volcano. Many things may affect the duration of a volcano's subaerial lifetime, among them the local weather conditions and the initial size of the volcano. As a result, the time required to erode a mature volcano ranges from ~3-25 Myr [*McDougall and Schmincke*, 1977; *Menard*, 1983; *Haggerty and Premoli Silva*, 1995], during which time the underlying lithosphere may subside. The time required to erode the volcano may be estimated by dating the oldest sediments on the volcano's top, but these data are available for only a few guyots in this study. Because of the large uncertainties associated with estimating erosion time we have chosen not to include it in our calculations. Instead, we note that that the thermal swells on which these volcanoes presumably formed were likely shallower than the

depths recorded by the guyots. The resulting bias is again toward taller seamounts.

A final factor that we consider is eustatic sea level change. Some volcanoes may have eroded flat during times of higher or lower sea level, which could alter predicted ocean depths by as much as 250 m [*Haq et al.*, 1987]. As shown in Figure 2, however, this difference is insufficient to explain most discrepancies relative to the depth of normal seafloor.

Because there are uncertainties associated with calculations of reef thickness, isostatic rebound, and depth to the erosional surface, we can evaluate the robustness of our results by looking at the volcano's maximum possible height. In this test we use only the depth to the volcano's highest point, ignoring all of the above effects and assuming zero seafloor sediment at the time the volcano formed. By using maximum height rather than height to slope break we can ascertain whether our contention that many intraplate volcanoes formed on shallow seafloor is simply a function of uncertainty in our height estimates. When maximum heights are used, we find that the heights of volcanoes in this study still average >900 m lower than would be predicted by the seafloor cooling curve of *Parsons and Sclater* [1977]. This confirms that even with the relative uncertainties associated with picking the depth to the erosional horizon on the volcano, the majority of volcanoes in this study formed on anomalously shallow seafloor.

In summary, the most important factor for which we were unable to correct is the change in seafloor depth between the time of eruption and the time of erosion to sea level. This factor, as well as the assumption that the seafloor was sediment-free at the time of volcano loading, has the effect of overestimating volcano height. Because we seek to model anomalously shallow regions, it is preferable to overestimate guyot heights and note that our thermal models may be lower bounds. The one factor that may lead to underestimates in height is the lack of isostatic correction for sediment loading on top of the guyot, where sediment thickness data were unavailable. We therefore believe that our finding that most of the volcano heights reflect anomalously shallow seafloor at the time of guyot formation is robust.

4. Models of Hotspot Thermal Anomalies

To characterize seafloor depth anomalies associated with intraplate volcanoes, we employ analytical models of lithosphere influenced by thermal anomalies. It is known that cooling oceanic lithosphere subsides at a rate approximately proportional to the square root of age [*Parsons and Sclater*, 1977; *Stein and Stein*, 1992]. Hotspots, however, commonly produce regions of anomalously shallow seafloor known as hotspot swells [*Crough*, 1983]. In previous studies, researchers have modeled the shallow paleodepths of hotspot seamounts using the concept of "thermal reset" [*Detrick and Crough*, 1978]. In this model the presence of a hotspot is thought to reset the thermal age of the lithosphere such that it behaves as if it was younger than its true age. *Crough* [1978] suggests that rejuvenated seafloor behaves as 25 Myr old lithosphere. *Clague* [1996] states that the 120 Myr old lithosphere beneath the youngest Emperor seamounts behaves as 40 Myr lithosphere, while the thermal age beneath the oldest Emperors is closer to 10 Myr. Other researchers suggest that the degree of thermal reset averages 40-45% of the actual lithospheric age [*Epp*, 1984; *Vogt and Smoot*, 1984]. No amount of age "reset," however, can account for seafloor depths shallower than normal ridge crests, which are commonly observed at hotspots occurring near mid-ocean ridges, such as Iceland, the Azores, and the Galapagos [e.g., *Ito and Lin*, 1995]. Indeed, many seamounts formed on crust younger than 20 Myr indicate current or paleo-water depths less than that of zero age lithosphere. We therefore develop a new model applicable for seafloor of all ages.

The cooling plate models presented by *Parsons and Sclater* [1977] and *Stein and Stein* [1992] are the basis for our model. We begin by calculating the vertical thermal structure of the lithosphere resulting from normal lithospheric cooling [*Parsons and Sclater*, 1977; *Stein and Stein*, 1992]. Then, at a specified time t_{hs}, we simulate the partial reheating and emplacement of an anomalously hot layer of mantle and calculate the associated depth anomaly (Figure 4). These models are analogous to models of *Sleep* [1994].

We begin by calculating the cooling of lithosphere for a normal plate. For ages <20 Myr, the lithosphere behaves as a cooling half-space and the depth is described [*Stein and Stein*, 1992] by

$$d(t) = d_r + 2\left(\frac{\kappa t}{\pi}\right)^{\frac{1}{2}} \frac{\rho \alpha T_0}{(\rho - \rho_w)}, \tag{1}$$

where d_r is the observed depth of zero age crust, κ is the thermal diffusivity, α is the volume coefficient of thermal expansion, T_o is the temperature of the asthenosphere and ρ = 3300 kg/m^3 and ρ_w = 1000 kg/m^3 are the densities of the mantle and sea water, respectively (Figure 4). The thermal diffusivity is given by $\kappa = k/\rho C_p$, where k is thermal conductivity and C_p is specific heat. For ages >20 Myr, the lithosphere cools as a plate of finite thickness A = 125 km and deepens according to

$$d(t) = d_r + d_s\left[1 - \left(\frac{8}{\pi^2}\right)\exp\left(\frac{-\kappa \rho^2 t}{A^2}\right)\right], \tag{2}$$

where d_s is the asymptotic depth of old lithosphere beneath the ridge and is given by

$$d_s = \frac{\alpha \rho T_o A}{2(\rho - \rho_w)}. \tag{3}$$

After *Parsons and Sclater* [1977], we assume values T_o = 1350°C, k = 3.138 W m^{-1} K^{-1}, C_p = 1.171 kJ kg^{-1} K^{-1}, and α = 3.28 + 10^{-5} K^{-1}. Like *Stein and Stein* [1992], we have defined our reference depth to be the ridge crest d_r, rather than asymptotic depth of old seafloor d_s.

At a given time t_{hs}, we simulate the injection of hot mantle of temperature T_{hs} beneath an arbitrarily chosen isotherm (1000°C) in the lithosphere. This results in a thinner "delaminated" lithosphere and anomalously low density asthenosphere with density

$$\rho_{hs} = \rho(1 - \alpha \Delta T), \tag{4}$$

where ΔT is the thermal anomaly $\Delta T = T_{hs} - T_o$. To determine the resulting seafloor depth, we assume the hot mantle layer and the partly delaminated lithosphere are in isostatic equilibrium with a compensation depth of 125 km. The mass of the partly delaminated lithosphere is calculated by first computing the temperature profiles of normal lithosphere according to

$$T(z) = T_o \mathrm{erf}\left[z(4\kappa t)^{-1/2}\right] \tag{5}$$

for ages < 20 Myr and

$$T(z) = T\left\{\frac{z}{A} + \sum_{n=1}^{\infty}\left[\left(\frac{2}{n\pi}\right)\exp\left(\frac{-n^2\pi^2\kappa T}{A^2}\right)\sin\left(\frac{n\pi z}{A}\right)\right]\right\} \quad (6)$$

for ages >20 Myr [*Parsons and Sclater*, 1977], where z is depth within the lithosphere. We then compute the mass per unit area M of the cooled lithosphere by converting these temperatures to density and integrating over the thickness z_l from the seafloor to the depth of the 1000°C isotherm. Finally, the depth of the uplifted seafloor is given by

$$d_{hs} = d_r + \frac{(\rho - \rho_{hs})(A + d_s) + (\rho_{hs} z_l) - M}{(\rho_w - \rho_{hs})} \quad (7)$$

(Figure 4). Thus, to apply this model to seamount height predictions, we compute the anomalous depth d_{hs} over a full range of lithospheric ages at the time of volcanism t_{hs} of 0-180 Myr. A t_{hs} of 0 Myr would correspond to the case of a hotspot occurring at a mid-ocean ridge crest, while greater values of t_{hs} correspond to hotspots occurring at older lithosphere.

Our choice of 1000°C as the isotherm below which the plume delaminates the lithosphere is consistent with the work of *Monnereau and Cazenave* [1990], who find that the plate beneath hotspot swells appears thinned to approximately the 900°-1000°C isotherm. *Sleep* [1994], however, suggests that vigorous convection is required to erode the base of the lithosphere to the 1000°C isotherm and argues that delamination to the 1250°C isotherm would be more likely. Higher values for this isotherm would require greater hotspot temperatures T_{hs} to account for the same uplift. For example, if we assume delamination to the 1000°C isotherm, a ~1000 m uplift can be explained by a hotspot temperature anomaly of 200°C. Alternatively, if we assume delamination at 1100°C, the same uplift would require a temperature anomaly of 300°C. Clearly, seafloor depth is influenced by a number of parameters, including delamination isotherm, plate thickness, and hotspot thermal anomaly. In our application to guyot heights the only parameter we vary is T_{hs}.

5. Comparison of Modeled and Observed Guyot Heights

We now compare observed guyot heights with models of various hotspot thermal anomalies (Figures 5 and 6). The resulting curves yield fits to observed data significantly closer than the normal seafloor cooling curve of *Parsons and Sclater* [1977]. We observe that while the heights of many intraplate volcanoes can be explained by the presence of a hotspot swell, some volcanoes show no height anomalies, suggestive of a nonhotspot origin. While some height variation may be due to changes in the thermal character of the source, some scatter is not predicted by this model and likely reflects local tectonic and geologic processes.

5.1. Hawaiian-Emperor Seamount Chain

We first focus on chains with the largest amount of height data over the widest ranges of seafloor age. The Hawaiian hotspot is among the most thoroughly analyzed in this study because volcanoes in that chain formed on lithosphere ranging in age from ~5-97 Myr (Figure 5a). Guyot heights range from just under 2200 m for the oldest Emperor seamount to over 5200 m for some of the atolls to the west of the main Hawaiian Islands. Although there is

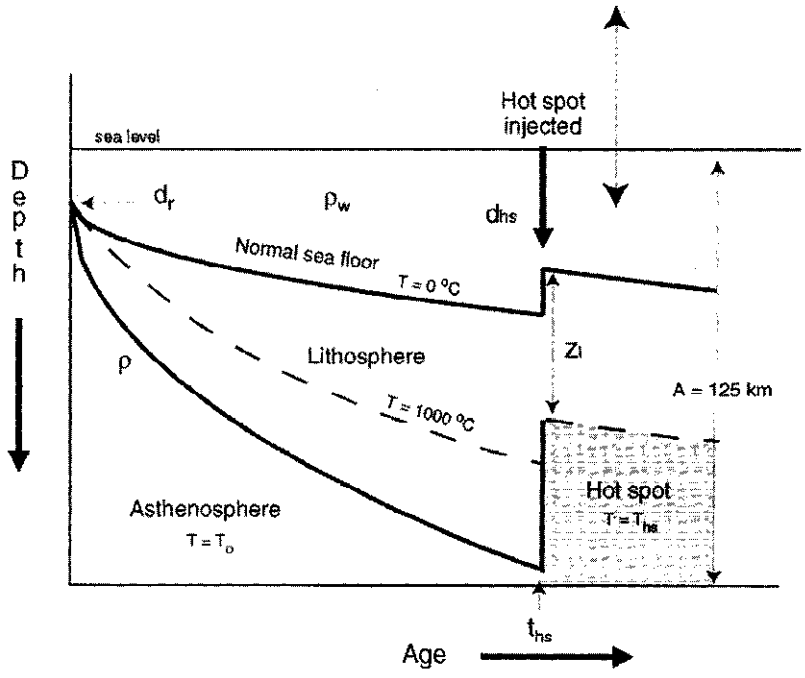

Figure 4. Cartoon of the thermal model. This model first allows lithosphere to cool normally. At some time t_{hs}, the injection of a hotspot is simulated by thinning the overlying lithosphere to an arbitrary "delamination isotherm" (1000°C), as labeled in the figure. At this time, the asthenosphere is replaced by material of temperature $T = T_{hs}$. The effect of this hotspot injection is the isostatic uplift of the lithosphere and the shoaling of the seafloor to a depth of d_{hs}.

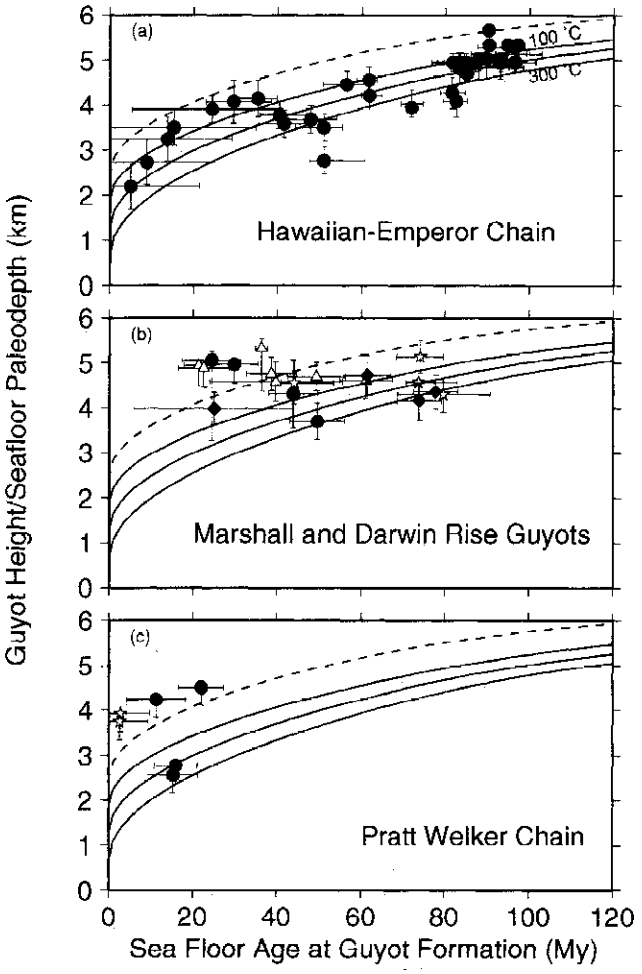

Figure 5. Seafloor depth curves modeled for (a) seamounts and islands of the Hawaiian-Emperor chain, (b) guyots and atolls of the Darwin Rise, and (c) seamounts of the Pratt-Welker chain. Dashed curves represents the "normal" seafloor depth of *Parsons and Sclater* [1977]. Solid curves are modeled predictions for thermal anomalies of 100°, 200°, and 300°C. In Figure 5b, symbols are as follows: stars, Marshall islands and guyots; triangles, Japanese or Geisha guyots; diamonds, Wake guyots; circles, Mid-Pacific Mountains. Stars in Figure 5c indicate seamounts in the Pratt-Welker chain which may have formed through normal mid-ocean ridge volcanics rather than by a hotspot [*Turner et al.*, 1980].

some scatter along the chain, it is clear that volcanoes which formed on younger crust preserve shallower paleodepths. For Hawaii we find a good fit with a thermal anomaly of 100°-200°C (Figure 7), consistent with the 100°-200°C anomaly invoked by *Von Herzen et al.* [1989]. Geochemical data constrain the thermal anomaly associated with the Hawaiian hotspot at ~200°C hotter than the ambient mantle [*Liu and Chase*, 1991; *Watson and MacKenzie*, 1991].

It is possible to explain the heights of all Hawaiian-Emperor volcanoes by invoking fluctuations in strength of the Hawaiian plume. However, thermal effects on the lithosphere are insufficient to account for all of the scatter within the Hawaiian-Emperor chain. For example, although Ojin and Jingu volcanoes rose from a common base and formed on the same age lithosphere, Jingu guyot is over 400 m taller than Ojin. While differences in erosion time might explain some height variation, the greater surface area of Ojin suggests it should have taken longer to erode and thus should be the taller of the two. Similarly, the flat top of Ninigi guyot sits nearly 400 m above the flat top of its neighbor, Godaigo. In the case of Ninigi and Godaigo, *Smoot* [1983] points out that the taller seamount has a more peaked top, seemingly less eroded. This feature suggests the presence of postsubmergence volcanics which could be confirmed with future sampling. A second possible cause of scatter is that the presence of other nearby volcanoes may produce lithospheric flexure that may perturb the depth at adjacent volcanoes. This effect may introduce uncertainties of the order of several hundred meters in paleo-water depth estimates [*Watts and ten Brink, 1989*]. Similar scatter is seen in guyots of the Darwin Rise (Figure 5b) and the Louisville chain (Figure 6a).

5.2. Darwin Rise Guyots

Figure 5b shows height versus age contrast for the guyots of the Darwin Rise, consisting of the Japanese, Wake, Marshall, and

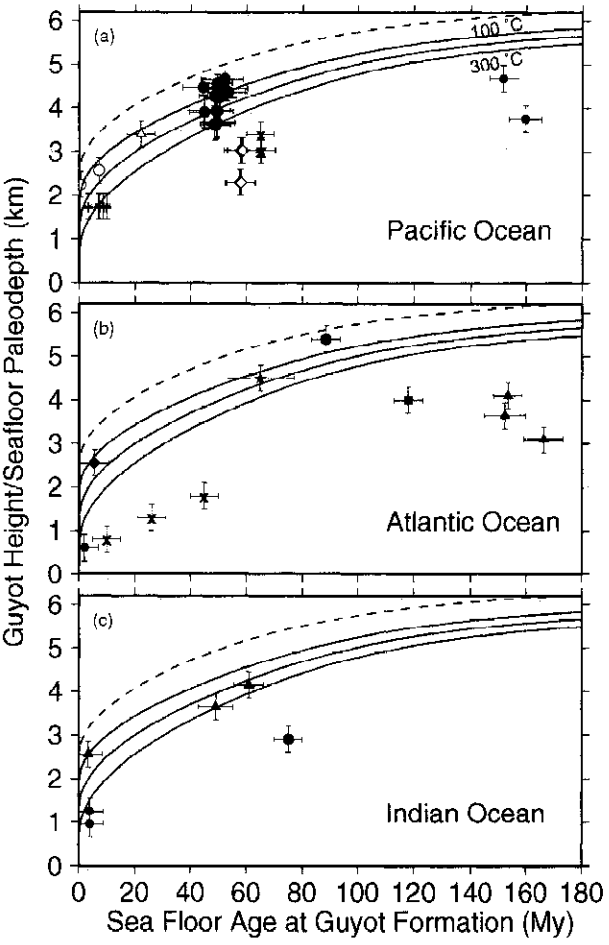

Figure 6. Approximate fit curves for seamounts and islands of the (a) Pacific, (b) Atlantic, and (c) Indian Oceans. Dashed curves represents the normal seafloor depth of *Parsons and Sclater* [1977]. Solid curves are modeled predictions for thermal anomalies of 100°, 200°, and 300°C. (a) Pacific ocean volcanoes not considered in Figure 5: hexagons, Caroline; circles, Easter; pluses, Galapagos; solid circles, Louisville; diamonds, Marquesas; triangles, Pitcairn; crosses, Society islands. (b) Atlantic Ocean islands: diamonds, Ascension; crosses, Azores; stars, Bermuda; hexagons, Bouvet; squares, Cape Verde; triangles, Canary islands; circles, Trindade. (c) Indian Ocean islands: hexagons, Amsterdam/St. Paul; circles, Prince Edward; triangles, Reunion.

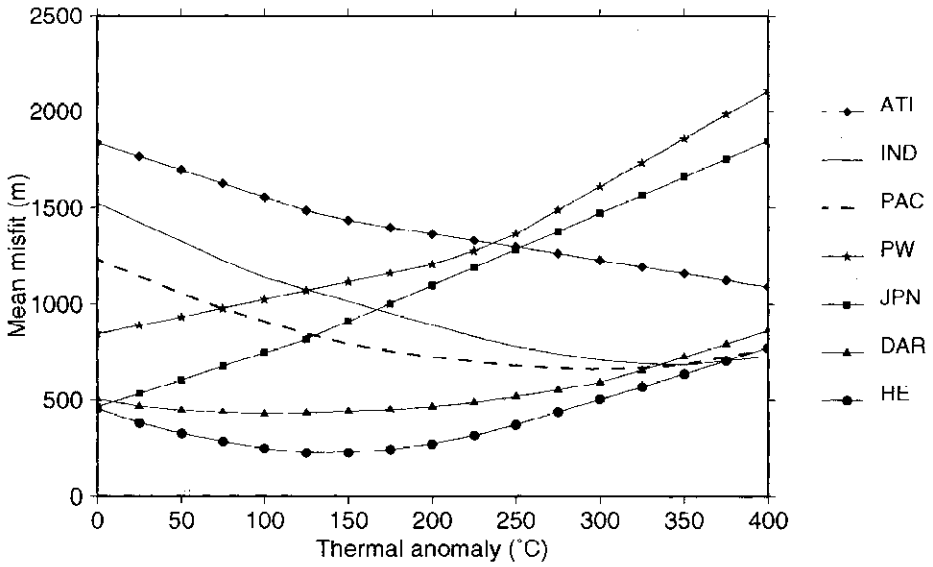

Figure 7. Average misfit for various hotspot groups for a range of thermal anomalies. While seamounts of the Hawaiian-Emperor chain and Darwin Rise exhibit a minimum misfit for thermal anomalies near 150°C, other volcanoes in the Atlantic, Indian, and Pacific Oceans suggest thermal anomalies nearer 300°C. Guyots of the Pratt-Welker and Japanese seamounts are better fit with no thermal anomaly. Hotspots and oceans are abbreviated as follows: HE, Hawaiian-Emperor; JPN, Japanese or Geisha guyots; DAR, Guyots of the Marshall, Wake and Mid-Pacific seamount groups, all located on or near the Darwin Rise; PW, Pratt-Welker guyots; PAC, Pacific Ocean); ATL, Atlantic Ocean; IND, Indian Ocean.

mid-Pacific groups. Because this region includes a number of different volcanic chains, we do not expect every seamount to fit a single curve. An approximate fit is made with a 100°-150°C thermal anomaly (Figure 7), although many seamounts in the chain lie closer to curves produced with 200° or 300°C anomalies and some require no thermal anomaly at all.

We make particular note of the heights of four guyots in the mid-Pacific mountains: Allison and Jacqueline guyots formed ~100 Ma (seafloor age of 43-50 Myr) while Resolution and Heezen guyots formed ~125 Ma (seafloor age of 23-30 Myr). Interestingly, the older guyots appear tall, requiring no thermal anomaly to explain their heights (Figure 5b). Allison and Jacqueline, however, are significantly lower in height than traditional cooling curves would predict, suggesting that these guyots formed over a thermal anomaly. This is consistent with the model presented by *McNutt et al.* [1990] that invokes a superswell-like thermal disturbance that affected the region ~120 Ma. This type of swell would uplift the seafloor such that the height of volcanoes formed after 120 Ma would be lower than the older volcanoes. In such a model, however, the older volcanoes would also be uplifted by the swell and should also record the new, shallower seafloor depth. The taller heights of the older mid-Pacific volcanoes thus remain unresolved. We note, however, that the depth to Resolution's erosional top is uncertain. While slope break is found at 1500 m depth, seismic reflection profiles of that Resolution show a reflection at ~2900 m depth, correlating with the drilled depth to volcanic basement [*Sager et al.*, 1993]. It is likely, therefore, that Resolution's slope break does not accurately represent the volcano's erosional horizon, and this is reflected in our error bars (Figure 5b).

The picture is made more complicated by the possibility of multiple stages of volcanism which may contribute to height variations. *Lincoln et al.* [1993] describe such a pattern of secondary volcanism for Wodejabato guyot in the Marshalls Islands. *Baker et al.* [1993] note that both Allison and Resolution guyots show evidence for having passed over more than one hotspot, an effect that would result in additional reheating and uplift of the seafloor. *Winterer et al.* [1993] also describe two cycles of uplift and subsidence for the mid-Pacific mountains.

A number of additional factors may have affected guyot heights among the Darwin Rise volcanoes. Most volcanoes within the Marshall, mid-Pacific, and Wake groups formed very near other volcanoes; thus the presence of nearby seamounts may have affected the heights of new ones, either by inducing lithospheric flexure or by serving as a base over which new material erupted. *Van Waasbergen and Winterer* [1993] note that many of the Marshall and mid-Pacific mountain guyots exhibit up to 300 m variation in the depth to slope break and attribute this, in part, to tilting in the presence of other seamounts.

In contrast to the other Darwin Rise volcano groups, the Japanese seamounts appear to have formed on lithosphere largely unaffected by reheating. This result supports the findings of *McNutt et al.* [1990], who conclude that several of the Japanese seamounts appear to have formed on "normal" depth lithosphere. We therefore contend that while most of the Marshall and mid-Pacific mountains appear to have formed at hotspots, another mechanism for melt generation must be invoked for the Japanese guyots.

5.3. Pratt-Welker Seamount Chain

The heights of most volcanoes in the Pratt-Welker chain in the Gulf of Alaska can be explained without the requirement of a thermal anomaly (Figure 5c). Consistent with these results, *Turner et al.* [1980] note that the Pratt-Welker seamounts appear to have undergone far less subsidence than that predicted by the thermal reset models of *Detrick and Crough* [1978] and further suggest that the lithosphere beneath these seamounts has undergone less reheating than suggested by *Crough* [1978]. However,

because our heights are based on maximum summit elevation, not slope break, the thermal anomaly suggested by our model curves is a lower bound. Additionally, *Turner et al.* [1980] note some uncertainty as to which of the seamounts in the chain formed at a hotspot and which formed due to normal mid-ocean ridge volcanism. Indeed, the seamounts thought to have formed at a ridge rather than over a hotspot (stars in Figure 5c) exhibit no height anomalies. In contrast to the rest of the volcanoes presented in this study, our models suggest that there was no anomalous uplift beneath the Japanese and Pratt-Welker guyots and that they did not form at hotspots.

5.4. Pacific Ocean Island, Atolls, and Guyots

Pacific seamounts other than those in the Hawaiian-Emperor, Marshall, and Pratt-Welker groups are plotted in Figure 6a where they are compared to model curves with thermal anomalies of 100°-300°C. Islands of the South Pacific superswell are particularly low. To explain the superswell, our model would require either a very high thermal anomaly (> 500°C), increased compensation depth, or delamination to a cooler (<1000°C) isotherm. The magnitude of this thermal anomaly suggests that local thermal uplift due to a single hotspot may be insufficient to describe the lower heights of the volcanoes. This is consistent with the findings of *McNutt and Judge* [1990] who invoke regional thermal uplift of the superswell due to anomalously thin lithosphere, associated with a regional-scale temperature anomaly.

The linear nature of the Louisville seamount chain makes it particularly interesting for this study. *Lonsdale* [1988] shows that through most of its history the Louisville hotspot has underlain lithosphere near 50 Myr old. One would therefore expect the Louisville guyots would rise to a common height, but this is not evident in the data. Thermal anomalies between 100° and 300°C, as shown in Figure 6a, can explain the heights of the Louisville guyots, but a large degree of scatter is still evident. When the Louisville guyots are plotted against age, it is apparent that older Louisville volcanoes formed on shallower seafloor, suggesting a hotter hotspot (Figure 8). A simple model might imply that the Louisville hotspot has cooled with time, and indeed, *Lonsdale* [1988] notes that the volumetric output of the Louisville hotspot appears to have waned in the last 25 Myr. Since 11 Ma, in fact, no Louisville volcanoes have breached sea level [*Lonsdale*, 1988].

5.5. Atlantic and Indian Ocean Islands

Figures 6b and 6c show data for volcanoes in the Atlantic and Indian Oceans. All of these volcanoes are still subaerial, and all heights lie far below the *Parsons and Sclater* [1977] age-depth curves even with a relatively high thermal anomaly of 300°C. The large amount of scatter in the heights of Atlantic and Indian Ocean volcanoes is unexplained by a simple hotspot model. Some possible explanations for the scatter are the proximity of some islands to continental crust (e.g., the Canary Islands) or the fact that some regions are thought to be underlain by thickened oceanic crust (e.g., the Azores platform). Thickening of the crust surrounding the volcanoes [*Ito and Lin*, 1995] may also explain the low heights of islands in the Galapagos Archipelago, none of which rises more than 1750 m above the surrounding seafloor.

6. Near-Ridge Origin of Meiji Seamount

Although the Hawaiian-Emperor hotspot chain is arguably the most studied in the world, little is known about its oldest member, Meiji seamount. Although few data exist regarding Meiji, this volcano was the subject of part of Deep Sea Drilling Project (DSDP) drilling leg 19 and was found to have a paleolatitude near to the present day Hawaiian hotspot [*Dalrymple et al.*, 1980], thus its origin is attributed to the Hawaiian hotspot. The data compiled here indicate that Meiji is only ~2200 m higher than the surrounding abyssal seafloor. Examination of Figure 2 suggests that the lowest guyots and islands formed near-ridge crests; in fact, most still sit on lithosphere < 10 Myr old. The trend in Figure 5a suggests that Meiji may have formed near a ridge. This possibility has important implications for plume-ridge interaction between the Hawaiian hotspot and one of the North Pacific spreading centers.

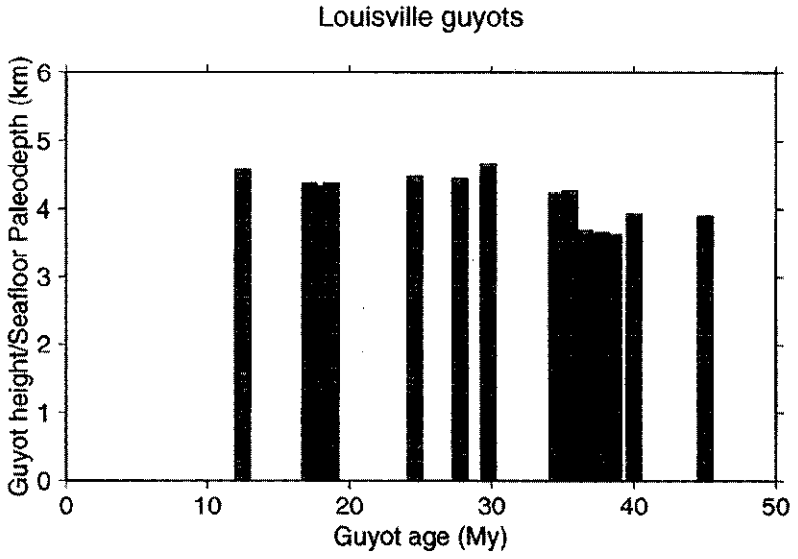

Figure 8. Height versus age for the Louisville guyots. Younger Louisville guyots are taller than older ones, suggesting that they formed on shallower lithosphere. Since 11 Ma, no Louisville volcanoes have breached sea level [*Lonsdale*, 1988]. This implies that the Louisville hotspot may be waning in intensity.

The age of the lithosphere on which Meiji seamount sits is poorly known. This lithosphere formed during the Cretaceous Quiet Zone and thus may have formed at one of several spreading centers (the Pacific-Izanagi, Pacific-Kula, or Pacific-Farallon). Evolutionary models, however, suggest that the lithospheric age is near 90 Myr [*Lonsdale*, 1988; *Rea and Dixon*, 1983; *Renkin and Sclater*, 1988; *Lonsdale et al.*, 1993]. An obvious constraint on the age of the lithosphere is the age of Meiji itself. The results of ODP leg 145 cite an age measurement of 81 Myr for a sample taken from the flank of Detroit tablemount, the next seamount to the ESE of Meiji [*Keller et al.*, 1995]. *Clague* [1996] suggests an age of 85 Myr for Meiji by calculating a linear age progression through only the most reliable age dates in the Hawaiian-Emperor chain. This age is consistent with the minimum age of ~72 Myr obtained from DSDP leg 19 [*Scholl and Creager*, 1973]. We therefore conclude that Meiji formed on ~5 Myr old lithosphere.

A near-ridge origin is also supported by the relatively low gravity signature around Meiji [*Sandwell and Smith*, 1997], a feature suggestive of isostatic compensation and hence formation on young lithosphere. Additionally, Meiji's morphology is considerably more subdued than that of the other, younger Emperor seamounts. In fact, Meiji bears morphological resemblance to oceanic plateaus such as Shatsky and Hess Rises, which are thought to have formed near ridges or triple junctions [*Watts et al.*, 1980; *Vallier et al.*, 1983; *Sager and Han*, 1993].

7. Conclusions

We constrain paleodepths of seafloor surrounding intraplate volcanoes by measuring the height of guyots, islands, and atolls in the Pacific, Atlantic, and Indian Oceans. We find that in most cases, guyot heights, and therefore seafloor paleodepths, are lower than predicted by normal seafloor cooling curves, indicating thermal uplift associated with hotspot swells. Isostatic models can explain most of the shallow depths with mantle thermal anomalies of 100°-300°C. These thermal models are consistent with previous geochemical and geodynamic analyses of hotspots. We find that guyot height generally increases with the age of the seafloor at the time of volcano formation. There is a ~2-3 km range in height observed throughout the overall trend which may be attributed to changes in hotspot strength and local geologic effects. Several volcanic chains, including the Japanese seamounts and Pratt-Welker chain, do not require any thermal uplift to explain their heights, suggesting that some intraplate volcanoes were not formed over hotspots.

The fact that there is a general age-height trend among the Hawaiian-Emperor guyots indicates that volcanoes have formed on progressively older lithosphere. The large-scale morphology and gravity anomaly of Meiji seamount bear a resemblance to oceanic plateaus, lending credence to the theory that they may have shared a similar origin: formation at a mid-ocean ridge.

Acknowledgments. We are grateful to Y. John Chen, W. Sager, and E. L. Winterer for helpful comments which greatly improved the clarity of this manuscript. We thank Loren Kroenke, John Sinton, and Brian Taylor for their advice and guidance on the project. J. C.-A. was funded in part by a University of Hawaii Geology and Geophysics department fellowship. G. I. was funded by the SOEST Young Investigator Fellowship. All figures in this paper were generated using GMT software [*Wessel and Smith*, 1995]. SOEST contribution number 4948.

References

Baker, P. E., P. R. Castillo, and E. Candliffe, Petrology and geochemistry of igneous rocks from Allison and Resolution guyots, sites 865 and 866, *Proc. Ocean Drill. Program Sci. Results*, *143*, 245-261, 1993.

Bergersen, D. D., Physiography and architecture of Marshall Islands guyots drilled during leg 144; geophysical constraints on platform development, *Proc. Ocean Drill. Program Sci. Results*, *144*, 561-583, Ocean Drilling Program, 1995.

Bonatti, E., Not so hot "hotspots" in the oceanic mantle, *Science*, *250*, 107-110, 1990.

Clague, D. A., The growth and subsidence of the Hawaiian-Emperor volcanic chain, in *The Origin and Evolution of Pacific Island Biotas, New Guinea to Eastern Polynesia: Patterns and Processes*, edited by A. Keast and S. E. Miller, pp. 35-50, SPB Acad., Amsterdam, 1996.

Clague, D. A., et al., Bathymetry of the Emperor seamounts, *Init. Rep. Deep Sea Drill. Proj.*, *55*, 845-849, 1980.

Crough, S. T., Thermal origin of mid-plate hot-spot swells, *Geophys. J. R. Astron. Soc.*, *55*, 451-469, 1978.

Crough, S. T., Hotspot swells, *Am. Rev. Earth Planet. Sci.*, *11*, 165-193, 1983.

Dalrymple, G. B., M. A. Lanphere, and J. H. Natland, K-Ar minimum age for Meiji Guyot, Emperor seamount chain, *Init. Rep. Deep Sea Drill. Proj.*, *55*, 677-681, 1980.

Davies, T. A., P. Wilde, and D. A. Clague, Koko Seamount: A major guyot at the southern end of the Emperor Seamounts, *Mar. Geol.*, 13, 311-321, 1972.

Detrick, R. S., and S. T. Crough, Island subsidence, hot spots, and lithospheric thinning, *J. Geophys. Res.*, *83*, 1236-1244, 1978.

Epp, D., Implications of volcano swell heights for thinning of the lithosphere by hotspots, *J. Geophys. Res.*, *89*, 9991-9996, 1984.

Haggerty, J. A., and I. Premoli Silva, Comparison of the origin and evolution of Northwest Pacific guyots drilled during leg 144, *Proc. Ocean Drill. Program Sci. Results*, *144*, 935-949, 1995.

Haq, B. U., J. Hardenbol, and P. R. Vail, Chronology of fluctuating sea levels since the Triassic, *Science*, *235*, 1156, 1987.

Hess, H. H., Drowned ancient islands of the Pacific Basin, *Am. J. Sci.*, *244*, 772-791, 1946.

Ito, G. T., and J. Lin, Mantle temperature anomalies along the present and paleoaxes of the Galapagos spreading center as inferred from gravity analyses, *J. Geophys. Res.*, *100*, 3733-3745, 1995.

Keller, R. A., R. A. Duncan, and M. R. Fisk, Geochemistry and Ar-Ar geochronology of basalts from ODP leg 145 (North Pacific transect), *Proc. Ocean Drill. Program Sci. Results*, *145*, 333-344, 1995.

King, S. D., and D. L. Anderson, An alternative mechanism of flood basalt formation, *Earth Planet. Sci. Lett.*, *136*, 269-279, 1995.

Ladd, H. S., J. I. Tracey Jr., and M. G. Gross, Drilling on Midway atoll, Hawaii, *Science*, *156*, 3778, 1088-1094, 1967.

Lincoln, J. M., P. Enos, G. F. Camoin, J. G. Ogg, and D. D. Bergersen, Geologic history of Wodejabato guyot, *Proc. Ocean Drill. Program Sci. Results*, *144*, 769-787, 1993.

Liu, M., and C. G. Chase, Evolution of Hawaiian basalts: A hotspot melting model, *Earth Planet. Sci. Lett.*, *104*, 151-165, 1991.

Lonsdale, P., Geography and history of the Louisville hotspot chain in the southwest Pacific, *J. Geophys. Res.*, *93*, 3078-3104, 1988.

Lonsdale, P., J. Dieu, and J. Natland, Posterosional volcanism in the Cretaceous part of the Hawaiian hotspot trail, *J. Geophys. Res.*, *98*, 4081-4098, 1993.

Ludwig, W. L., and R. E. Houtz, Isopach map of sediments in the Pacific Ocean basin and marginal sea basins, Am. Assoc. of Petroleum Geol., Tulsa, Okla., 1979.

McDougall, I., and H. U. Schmincke, Geochronology of Gran Canaria, Canary Islands; age of shield building volcanism and other magmatic phases, *Bull. Volcanol.*, *40* (1), 57-77, 1977.

McNutt, M. K., and A. V. Judge, The superswell and mantle dynamics beneath the South Pacific, *Science*, *248*, 969-975, 1990.

McNutt, M. K., and H. W. Menard, Lithospheric flexure and uplifted atolls, *J. Geophys. Res.*, *83*, 1206-1212, 1978.

McNutt, M. K., et al., The Darwin Rise: A Cretaceous superswell?, *Geophys. Res. Lett.*, *17*, 1101-1104, 1990.

McNutt, M. K., D. W. Caress, J. Reynolds, K. A. Jordahl, and R. A Duncan, Failure of plume theory to explain midplate volcanism in the southern Austral Island, *Nature*, *389*, 479-482, 1997.

Menard, H. W., Insular erosion, isostasy and subsidence, *Science*, *220*, 913-918, 1983.

Monnereau, M., and A. Cazenave, Depth and geoid anomalies over oceanic hotspot swells: A global survey, *J. Geophys. Res.*, *95*, 15,429-15,438, 1990.

Muller, R. D., et al., Digital isochrons of the world's ocean floor, *J. Geophys. Res.*, *102*, 3211-3214, 1997.

Parsons, B., and J. G. Sclater, An analysis of the variation of ocean floor bathymetry and heat flow with age, *J. Geophys. Res.*, *82*, 803-827, 1977.

Premoli Silva, I., et al., *Proceedings of the Ocean Drilling Program Initial Reports*, vol. 144, Ocean Drill. Program, College Station, Tex., 1993.

Pringle, M. S., and R. A. Duncan, Radiometric ages of basaltic lavas recovered at sites 865, 866 and 869, *Proc. Ocean Drill. Program Sci. Results*, *143*, 277-283, 1993.

Pringle M. S. and R. A. Duncan, Radiometric ages of basement lavas recovered at Lo-En, Wodejabato, MIT and Takuyo-Daisan guyots, Northwestern Pacific Ocean, *Proc. Ocean Drill. Program Sci. Results*, *144*, 547-557, 1995.

Rea, D. K., and J. M. Dixon, Late Cretaceous and Paleogene tectonic evolution of the North Pacific Ocean, *Earth Planet. Sci. Lett.*, *65*, 145-166, 1983.

Renkin, M. L., and J. G. Sclater, Depth and age in the North Pacific, *J. Geophys. Res.*, *93*, 2919-2935, 1988.

Sager, W. W., Seamount age estimates from paleomagnetism and their implications, in *Geology and Offshore Mineral Resources of the Central Pacific Basin*, edited by. B. H. Keating and B. R. Bolton, pp. 27-37, Springer-Verlag, New York, 1992.

Sager, W. W., and H. C. Han, Rapid formation of the Shatsky Rise oceanic plateau inferred from its magnetic anomaly, *Nature*, *364*, 610-613, 1993.

Sager, W. W., et al., *Proceedings of the Ocean Drilling Program, Initial Reports*, vol. 143, Ocean Drilling Program, College Station, Tex., 1993.

Sandwell, D. T., and W. H. F. Smith, Marine gravity anomaly from Geosat and ERS 1 satellite altimetry, *J. Geophys. Res.*, *102*, 10,039-10,054, 1997.

Sandwell, D. T., E. L. Winterer, J. Mammerickx, R. A. Duncan, M. A. Lynch, D. A. Levitt, and C. L. Johnson, Evidence for diffuse extension of the Pacific plate from Pukapuka ridges and cross-grain gravity lineations, *J. Geophys. Res.*, *100*, 15,087-15,099, 1995.

Scholl, D. W., and J. J. Creager, Geologic synthesis of leg 19 (DSDP) results: Far north Pacific, and Aleutian Ridge, and Bering Sea, *Init. Rep. Deep Sea Drill. Prog.*, *19*, 897-913, 1973.

Scholl, D. W., J. R. Hein, M. Marlow, and E. C. Buffington, Meiji sediment tongue: North Pacific evidence for limited movement between the Pacific and North American plates, *Geol. Soc. Amer. Bull.*, *88*, 1567-1576, 1977.

Simkin, T., Origin of some flat-topped volcanoes and guyots, *Mem. Geol. Soc. Amer.*, *132*, 183-193, 1972.

Sleep, N. H., Lithospheric thinning by midplate mantle plumes and the thermal history of hot plume material ponded at sublithospheric depths, *J. Geophys. Res.*, *99*, 9327-9343, 1994.

Smoot, N. C., Guyots of the mid-Emperor chain mapped with multi-beam sonar, *Mar. Geol.*, *47*, 153-163, 1982.

Smoot, N. C., Ninigi and Godaigo seamounts: Twins of the Emperor chain by multi-beam sonar, *Mar. Geol.*, *98*, T1-T5, 1983.

Smoot, N. C., Guyot and seamount morphology and tectonics of the Hawaiian-Emperor elbow by multi beam sonar, *Mar. Geol.*, *64*, 203-215, 1985.

Stein, C. A., and S. Stein, A model for the global variation in oceanic depth and heat flow with lithospheric age, *Nature*, *359*, 123-129, 1992.

Turner, D. L., R. D. Jarrard, and R. B. Forbes, Geochronology and origin of the Pratt-Welker seamount chain, Gulf of Alaska: A new pole of rotation for the Pacific Plate, *J. Geophys. Res.*, *85*, 6547-6556, 1980.

Vallier, T. L., W. E. Dean, and D. K. Rea, Geologic evolution of Hess Rise, central North Pacific Ocean, *Geol. Soc. Amer. Bull.*, *94*, 1430-1437, 1983.

Van Waasbergen, R. J., and E. L. Winterer, Summit geomorphology of western pacific guyots, in *The Mesozoic Pacific: Geology, Tectonics and Volcanism, Geophys. Monogr. Ser.*, vol. 77, pp. 335-366, AGU, Washington D. C., 1993.

Vogt, P. R., and N. C. Smoot, The Geisha Guyots: multibeam bathymetry and morphometric interpretation, *J. Geophys. Res.*, *89*, 11,085-11,107, 1984.

Von Herzen, R. P., M. J. Cordery, R. S. Detrick, and C. Fang, Heat flow and the thermal origin of hot spot swells: The Hawaiian swell revisited, *J. Geophys. Res.*, *83*, 13,783-13,799, 1989.

Watson, S., and D. McKenzie, Melt generation by plumes: A study of Hawaiian volcanism, *J. Petrol.*, *32*, 501-537, 1991.

Watts, A. B., and U. S. ten Brink, Crustal structure, flexure, and subsidence history of the Hawaiian islands, *J. Geophys. Res.*, *94*, 10,473-10,500, 1989.

Watts, A. B., J. H. Bodine, and N. M. Ribe, Observations of flexure and the geological evolution of the Pacific Ocean basin, *Nature*, *283*, 532-537, 1980.

Wessel, P., and W. H. F. Smith, New version of the Generic Mapping Tools released, *EOS Trans. AGU*, *76* (33), 329, 1995.

Weinrebe, W., C. Kopp, and J. O'Connor, High resolution morphology of Daikakuji seamount: Hawaiian-Emperor chain bend (abstract), *EOS Trans. AGU*, *78* (46), F726, Fall Meet. Suppl., 1997.

Winterer, E. L., Sediment thickness map of the Northeast Pacific, in *The Eastern Pacific Ocean and Hawaii*, vol. N, *The Geology of North America*, edited by E. L. Winterer, D. M. Hussong, and R. W. Decker, Boulder, Colorado, *Geol. Soc. Am.*, 1989.

Winterer, E. L., and W. W. Sager, Synthesis of drilling results from the Mid-Pacific Mountains: Regional context and implications, *Proc. Ocean Drill. Program Sci. Results*, *143*, 497-535, 1993.

Winterer, E. L., et al., Cretaceous guyots in the Northwest Pacific: An overview of their geology and geophysics, in *The Mesozoic Pacific: Geology, Tectonics, and Volcanism*, Geophys. Monogr. Ser., vol. 77, pp. 307-334, AGU, Washington D. C., 1993.

J. Caplan-Auerbach, F. Duennebier, and G. Ito, Department of Geology and Geophysics, University of Hawaii at Manoa, 160 East-West Road, Honolulu, HI 96822. (jackie@soest.hawaii.edu)

(Received October 2, 1998; revised September 13, 1999;
accepted October 28, 1999.)